Molecular Crystals and Liquid Crystals
Publication details, including instructions for authors and subscription information:
http://www.tandfonline.com/loi/gmcl16

^{13}C NMR Study of Molecular Dynamics in Twisted Nematic Phases

Metka Luzar [a] , Bojan Lozar [a] , Robert Blinc [a] & J. William Doane [b]

[a] J. Stefan Institute, E. Kardelj University of Ljubljana, 61000, Ljubljana, Yugoslavia

[b] Department of Physics, Kent State University, Kent, Ohio, USA

Version of record first published: 17 Oct 2011.

To cite this article: Metka Luzar , Bojan Lozar , Robert Blinc & J. William Doane (1984): ^{13}C NMR Study of Molecular Dynamics in Twisted Nematic Phases, Molecular Crystals and Liquid Crystals, 113:1, 291-301

To link to this article: http://dx.doi.org/10.1080/00268948408071690

Mol. Cryst. Liq. Cryst., 1984, Vol. 113, pp. 291-301
0026-8941/84/1134-0291/$20.00/0

Printed in the United States of America

^{13}C NMR STUDY OF MOLECULAR DYNAMICS IN TWISTED NEMATIC PHASES

METKA LUZAR, BOJAN LOŽAR, ROBERT BLINC
J. Stefan Institute, E. Kardelj University of Ljubljana, 61000 Ljubljana, Yugoslavia
J. WILLIAM DOANE
Department of Physics, Kent State University, Kent, Ohio, USA

Abstract ^{13}C NMR spectral patterns over the full temperature range of the twisted nematic phase of the binary mixture of MBBA (methoxybenzylidene butylaniline) and chiral MBMBA (methoxybenzylidene 2–methyl butylaniline) are evaluated in terms of the molecular motions averaging the chemical shift tensors of the ^{13}C nuclei. The measurements allowed for a determination of the molecular self–diffusion constant along the pitch axis of the helicoidal structure.

I. INTRODUCTION

The nematic liquid crystal, which is normally uniaxial can be twisted by an addition of an optically active or chiral material. The helical twisted arrangement of the molecules is defined by the pitch axis. The material discussed in this paper is a very common nematic compound MBBA (methoxybenzylidene butylaniline), to which 12 wt% of the chiral material MBMBA (methoxybenzylidene 2–methyl butylaniline) is added. The latter has been made chiral by the addition of a branched CH_3 methyl group in the β carbon position of the alkyl chain of MBBA[1] (Fig. 1).

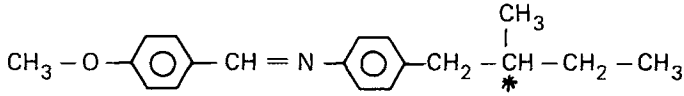

FIGURE 1. Optically active methoxybenzylidene 2–methyl butylaniline (MBMBA)

In this paper we wish to present the results of a ^{13}C NMR study of molecular ordering and dynamics in the twisted nematic phase of the MBBA – MBMBA mixture.

II. EXPERIMENTAL TECHNIQUE

The ^{13}C NMR spectra have been measured on a pulsed Fourier transform NMR spectrometer using a superconducting magnet. The ^{13}C and ^{1}H Larmor frequencies were 67,9 MHz and 270 MHz, respectively. In the nematic phase the Pines–Gibby–Waugh proton–^{13}C cross polarization technique has been used[2]. All chemical shifts were measured with respect to TMS.

III. ^{13}C SPECTRA

The temperature dependence of the ^{13}C chemical shifts of the MBBA–MBMBA mixture in the isotropic and nematic phases has been measured. In the isotropic phase the positions of all chemically non–equivalent ^{13}C lines coincide with those in pure MBBA published before[3] except for the appearance of an additional line corresponding to the carbon in the chiral CH_3 group of MBMBA. On cooling the sample from the isotropic phase a phase transition appears at 39°C and powder spectral patterns result in contrast to what is observed in pure nematic MBBA[3].

In view of the fast random rotational and translational molecular motions one observes in the *isotropic phase* only the isotropic part of the ^{13}C chemical shift tensor $\underline{\sigma}$, $\sigma_i = \frac{1}{3} \mathrm{Tr}\, \underline{\sigma}$, whereas the anisotropic part is averaged out to zero.

When the sample is cooled from the isotropic into the *twisted nematic* phase a helical twisted arrangement of the elongated molecules appears. The pitch axis of the twisted structure is aligned perpendicular to the direction of the external magnetic field (Fig. 2). The chemical shift tensor is no longer isotropic. It is averaged by the following molecular motions:

- fast molecular rotations around the long molecular axis, and
- fluctuations of the long molecular axis around the molecular director $\vec{N}$ which follows a helical arrangement with the helicoidal axis perpendicular to the direction of the applied magnetic field $\vec{H}$.

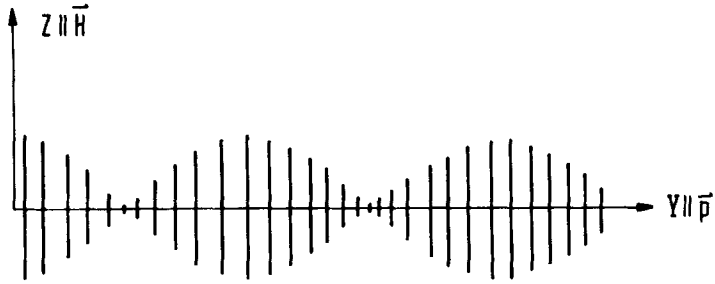

FIGURE 2. Schematic representation of the helical twisted arrangement of preferential orientation of molecular long axes in the twisted nematic phase. The pitch axis $\vec{p}$ is perpendicular to the magnetic field $\vec{H}$.

The component of the chemical shift tensor in the direction of the external magnetic field $\sigma = <\sigma_{ZZ}> \equiv <\sigma_H>$ is obtained as:

$$\sigma = \sigma_i + \frac{2}{3}[\sigma_{zz} - \frac{1}{2}(\sigma_{xx} + \sigma_{yy})]\, S_{zz} + \\ + \frac{1}{3}(\sigma_{xx} - \sigma_{yy})(S_{xx} - S_{yy})\,(\frac{3}{2}\cos^2\theta - \frac{1}{2}) \qquad (1)$$

where

$$S_{zz} = S = <\frac{3}{2}\cos^2\beta - \frac{1}{2}> \qquad (2a)$$

measures the amount of "nematic" ordering of the long molecular axis around the molecular director $\vec{N}$, and

$$S_{xx} - S_{yy} = \frac{3}{2}<\sin^2\beta\,\cos 2\varphi> \qquad (2b)$$

measures the asymmetry in the fluctuations of the long molecular axis around the x and y axis. The molecular fixed frame x, y, z and the "director" coordinate frame x', y', z', with the z'axis parallel to the molecular director $\vec{N}$, are illustrated in Fig. 3. The angle β (t) measures the fluctuations of the long molecular axis around $\vec{N}$. The angle φ(t) measures the orientation of the short molecular axis as the molecule rotates around its long axis. The molecular director $\vec{N}$ makes an angle θ with the direction of $\vec{H}$. The angle θ changes along the direction of

the pitch axis which is parallel to the Y axis of the fixed laboratory frame X,Y, Z, with Z axis parallel to $\vec{H}$ (Fig. 4).

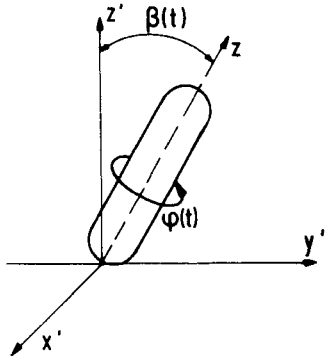

FIGURE 3. Relation between the molecular frame x, y, z and the "director" frame x', y', z' ∥ $\vec{N}$.

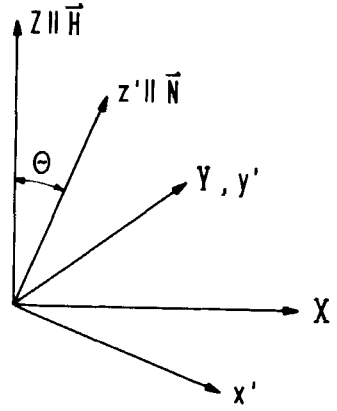

FIGURE 4. Relation between the "director" frame x', y', z' ∥ $\vec{N}$ and the laboratory frame X, Y, Z ∥ $\vec{H}$.

The value of $\sigma_{xx} - \sigma_{yy}$ is of the order of 100 ppm for the aromatic carbons. This difference is effectively averaged out by fast conformational changes, like 90° flips of benzene rings around the para axis, so that $\sigma_{xx} \cong \sigma_{yy}$. Furthermore $(S_{xx} - S_{yy})$ is quite small as opposed to the values for S_{zz} in nematics. Expression (1) thus simplifies to:

$$\sigma = \sigma_i + \frac{2}{3} S (\sigma_{\parallel} - \sigma_{\perp})(\frac{3}{2} \cos^2 \theta - \frac{1}{2}) \tag{3}$$

where $\sigma_{\parallel} = \sigma_{zz}$ is the component along the direction of the long molecular axis and $\sigma_{\perp} = \frac{1}{2}(\sigma_{xx} + \sigma_{yy})$ is the average component in the x − y plane.

If $I(\sigma)$ is the intensity of the NMR line at the chemical shift σ and $p(\theta)\, d\theta$ is the probability of finding the tensor orientation in the range between the angle θ and $\theta + d\theta$, we may write:

$$I(\sigma)\, d\sigma = p(\theta)\, d\theta \tag{4}$$

In the case of a uniform distribution of the angle θ in the plane perpendicular to the pitch axis, the probability density is $p(\theta) = \frac{1}{2\pi}$. Thus we get:

$$I(\sigma) = \frac{1}{2\pi} \left| \frac{d\theta}{d\sigma} \right| \tag{5}$$

Using Eq. (3) we arive at the line shape function as

$$I(\sigma) = \frac{1}{4\pi K} \left[\left(1 + \frac{\sigma - \sigma_i}{K} \right) \left(2 - \frac{\sigma - \sigma_i}{K} \right) \right]^{-1/2} , \tag{6a}$$

where

$$K = \frac{1}{3} S(\sigma_{\parallel} - \sigma_{\perp}) . \tag{6b}$$

Schematic representation of the theoretical line shape is plotted in Fig. 5. Usually a residual line broadening is taken into account by a convolution of $I(\sigma)$ with a broadening function (Lorentzian or Gaussian). The resonance line shape has edge singularities at

$$\sigma = \sigma_i + 2K , \quad \text{i.e.} \quad \theta = 0^{\circ} \tag{7a}$$

$$\sigma = \sigma_i - K , \quad \text{i.e.} \quad \theta = 90^{\circ} \tag{7b}$$

and the minimum at $\sigma = \sigma_i + \frac{1}{2} K$.

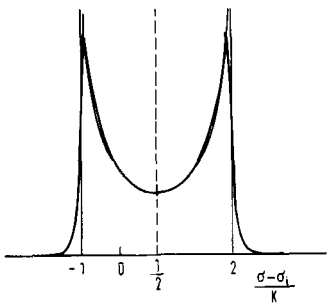

FIGURE 5. Schematic representation of the theoretical line shape according to Eqs. 6. Solid line is a convolution of a theoretical curve with Lorentzian broadening function.

If only the above molecular motions averaged the chemical shift tensor the observed line width of each nonequivalent ^{13}C nucleus would depend on the chemical shift anisotropy $\Delta\sigma = \sigma_{\parallel} - \sigma_{\perp}$ of the relevant nucleus and the order parameter S. A major obstacle for the use of ^{13}C spectroscopy in liquid crystal studies has been the lack of precise knowledge of ^{13}C chemical shift tensors and their orientation. This situation has been somewhat changed recently because of the widespread use of ^{13}C – proton double resonance that has provided a wealth of ^{13}C chemical shift tensors for different compounds and shown that ^{13}C tensors for a specific molecular group can be to a rather good approximation transferred from one compound to another. This is the approach used in this paper. Since the ^{13}C chemical shift tensors for MBBA are not known, we have used the data from related solid compounds containing the relevant ^{13}C groups. For the aromatic carbons one obtains from the published data[4] on the eigenvalues of $\underline{\sigma}$ and the orientations of the principal axes of $\underline{\sigma}$ the following values for $\Delta\sigma$: $\Delta\sigma^{(o)} = \sigma_{\parallel}^{(o)} - \sigma_{\perp}^{(o)} = 52$ ppm for the carbons at the ortho – positions and $\Delta\sigma^{(p)} = \sigma_{\parallel}^{(p)} - \sigma_{\perp}^{(p)} = 142$ ppm for the carbons at the para–sites. For an accurate determination of $\sigma_{\parallel} - \sigma_{\perp}$ the angle $\gamma \cong 10^{o}$ between the para–axis and the rotation axis of the molecule has also been taken into account[5]. Because of the large values of linewidths the lines of different carbons overlap and the obtained spectra are the superpositions of all the nonequivalent ^{13}C lines as shown on Fig. 6a. Most of the line edge–singularities can be distinguished. Clearly, the linewidths of the carbons at the para-positions are larger than those of the ortho carbons because of the larger value of $\Delta\sigma$ and the same S for all the carbons on the aromatic ring. The linewidths of the aliphatic carbons are significantly smaller because of smaller values of S and the smaller anisotropy, $|\Delta\sigma| < 30$ ppm[6]. In view of the latter the accuracy of the ^{13}C measurements is here not very high.

The spectral pattern corresponding to the aromatic carbons and the ^{13}C in the central C = N group that appears at lower magnetic fields (i.e. higher chemical shifts with respect to TMS) and the lines corresponding to the aliphatic carbons that show up at higher magnetic fields (i.e. lower chemical shifts with respect to TMS), are divided by a single narrow line at 55 ppm with respect to TMS which is due to the carbon in the $O–CH_3$ group. The change in the

position of the line at the isotropic–twisted nematic transition is negligeable, which indicates that the average angle between the O–CH_3 axis and the molecular director $\vec{N}$ is close to the "magic angle" (54,7°).

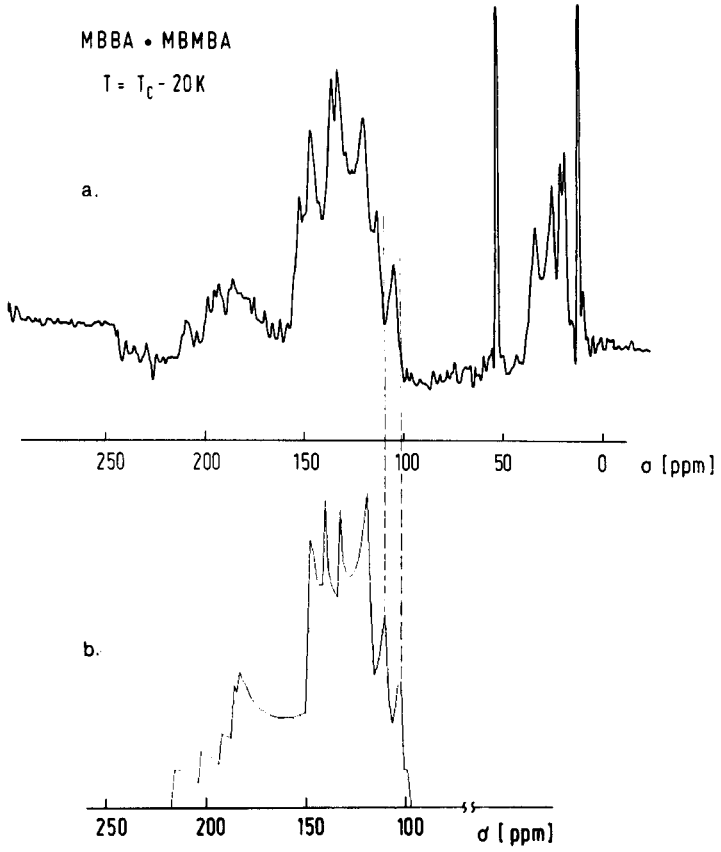

FIGURE 6. a. ^{13}C NMR spectra in the twisted nematic phase of the MBBA – MBMBA mixture at $T = T_c - 20$ K.
b. Calculated spectral pattern at the same reduced temperature T/T_c according to Eqs. 6.

Fig. 6b shows the calculated spectral pattern corresponding to the aromatic carbons in the ortho-and para—positions and the carbon in the central C = N group which should be compared with the measured one. The values of $\Delta\sigma = \sigma_{\parallel} - \sigma_{\perp}$ were calculated from the published data as shown before, the values of S for the relevant carbons were taken from the ^{13}C published data in a pure nematic MBBA[3] considering the same reduced temperature. We believe that there is no significant difference between the values of S in the untwisted sample and those in the twisted sample, referring to the central part of the molecule. The comparison of the measured and the calculated spectral patterns clearly demonstrates the existence of significant differences in the positions of the line singularities corresponding to the same ^{13}C nucleus. These deviations appear to be rather small but they can be a result of some overlooked molecular motions that time average the chemical shift tensor. In the twisted structure self—diffusion of the molecules along the pitch axis may further average the $\underline{\sigma}$ tensor during the time scale of the NMR experiment.

IV. EFFECTS OF SELF—DIFFUSION

In the case where the pitch axis $\vec{p}$ is perpendicular to $\vec{H}$ molecular diffusion along the direction of the pitch axis changes the orientation of the molecules with respect to $\vec{H}$. During the time scale of the experiment the chemical shift tensor is therefore further time averaged since θ in Eq. (3) varies. For simplicity let us rewrite Eq. (3) as:

$$\sigma = \sigma_i + \frac{K}{2}(1 + 3\cos 2\theta) \tag{8}$$

A molecule that is situated at a time t = 0 at an arbitrary position y_o on the pitch axis is brought by the diffusion to a new position y on the pitch axis at a time t with the probability $P(y_o, y, t)$ that can be described by the Gaussian function[7]:

$$P(y_o, y, t) = \frac{1}{\sqrt{4\pi Dt}} \exp\left(-\frac{(y - y_o)^2}{4Dt}\right) \tag{9}$$

where D is the self—diffusion constant along the pitch axis. If the

helix is undistorted by the magnetic field there is a linear relationship between y and θ [8], which allows one to write:

$$(y - y_o) = \frac{p_o}{2\pi}(\theta - \theta_o) \tag{10}$$

where p_o is the pitch length. Therefore for a discrete time t, Eq.(8) must be averaged over θ as:

$$<\sigma(\theta_o, t)>_\theta = \int_{-\infty}^{+\infty} P(\theta_o, \theta, t)\,\sigma(\theta)\,d\theta =$$

$$= \sigma_i + \frac{K}{2}(1 + 3R\cos 2\theta_o) \tag{11}$$

where

$$R = \exp\left(-\frac{16\pi^2 Dt}{p_o^2}\right) \tag{12}$$

Furtheron $<\sigma(\theta_o, t)>_\theta$ must be averaged over the time t when the diffusion takes place:

$$<\sigma(\theta_o, \tau)>_{\theta,t} = \frac{1}{\tau}\int_o^\tau \sigma(\theta_o, t)\,dt =$$

$$= \sigma_i + \frac{K}{2}(1 + 3\tilde{R}\cos 2\theta_o)\,, \tag{13}$$

where

$$\tilde{R} = \frac{p_o^2}{16\pi^2 D\tau}\left(1 - \exp\left(-\frac{16\pi^2 D\tau}{p_o^2}\right)\right)\,. \tag{14}$$

τ is the averaging time associated with each nonequivalent ^{13}C line. It is basically the length of the free–induction decay for each ^{13}C site. τ^{-1} will be proportional to $\tau^{-1} \propto (\sigma_\parallel - \sigma_\perp) \propto \sigma - \sigma_i = 2K$ at $\theta = 0^o$ obtained from the untwisted sample. Eq. (13) can be considered as an average component of the chemical shift tensor along $\vec{H}$ over the time interval from t = 0 to t = τ. It was shown [8] that this is a good approximation that one can use to obtain singularities which arise in the spectral pattern. It is noted that Eq. (14) has proper limits for D = 0 and ∞.

To obtain the spectral pattern one must take into account the

uniform distribution of θ_o in the plane perpendicular to $\vec{p}$. Using Eqs. (4), (5) and (13) one obtains:

$$I(\sigma) = \frac{1}{2\pi K}\left[(3\tilde{R}+1) - \frac{2(\sigma-\sigma_i)}{K}\right]\left[(3\tilde{R}-1) + \frac{2(\sigma-\sigma_i)}{K}\right]^{-1/2} \tag{15}$$

Schematic representation of this line shape is the same as the one plotted on Fig. 5 but with the singularities that appear at:

$$\sigma = \sigma_i + \frac{K}{2}(3\tilde{R}+1), \quad \text{i.e.} \quad \theta_o = 0^o \tag{16a}$$

$$\sigma = \sigma_i + \frac{K}{2}(1-3\tilde{R}), \quad \text{i.e.} \quad \theta_o = 0^o . \tag{16b}$$

From the shifts of the above edge – singularities from the positions of the lines in the untwisted sample [3] at the same reduced temperature T/T_c we measure the values of $\tilde{R}$, from which the values of $D\tau/p_o^2$ for different ^{13}C sites can be determined. p_o is found [9] to be only weakly temperature dependent and is approximately 2 μm at our

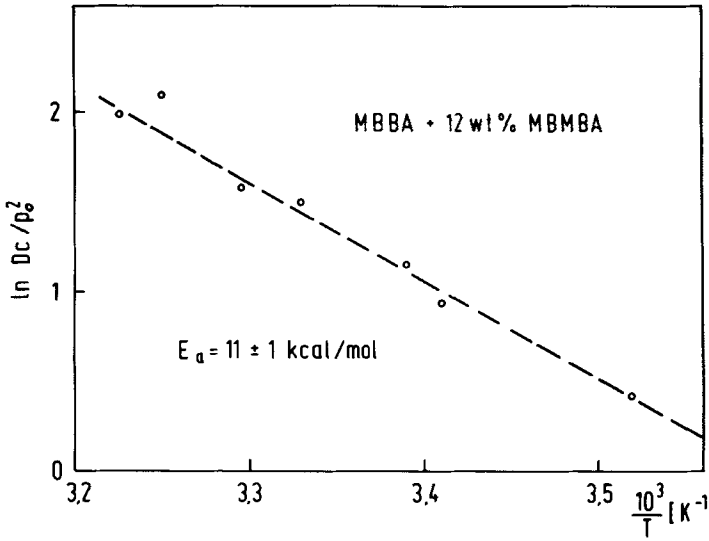

FIGURE 7. Plot of ln Dc/p_o^2 versus reciprocal temperature, where $c = \tau|\sigma - \sigma_i|$, for the carbons at the para-sites of the aromatic ring.

concentration of MBMBA. τ follows the T – dependence of $(\sigma - \sigma_i)^{-1}$ of the untwisted MBMBA. The self–diffusion is thermally activated and follows $D = D_o e^{-E_a/kT}$. In Fig. 7 we have plotted ln (Dc/p_o^2) versus reciprocal temperature T^{-1}, where $c = \tau |\sigma - \sigma_i|$, for the carbons at the para – sites. Since $c = \tau |\sigma - \sigma_i|$ is temperature independent the slope of the line, drawn by a least squares fit, gives an activation energy. From the aromatic carbons the average activation energy for the self–diffusion along the pitch axis is obtained as $E_a = 11 \pm 1$ kcal/mol which is in reasonably good agreement with ^{2}D – measurements[9] on a similar mixture. The values of the self–diffusion constant along the pitch axis are estimated to range from $D = 6 \cdot 10^{-8}$ cm^2/s to $D = 3 \cdot 10^{-7}$ cm^2/s throughout the entire twisted nematic phase.

REFERENCES:

1. J.W. Doane, Z. Yaniv, G. Chidichimo and N. Vaz, Proc. of 7th Ampere Int. Summer School, Portorož, 1982.
2. A. Pines, M.G. Gibby, and J.S. Waugh, J. Chem. Phys., 59, 569 (1979).
3. A. Pines, J.J. Chang, Phys. Rev. A, 10, 946 (1974).
4. A. Pines, M.G. Gibby and J.S. Waugh, Chem. Phys. Lett., 15, 373 (1972); S. Pausak, A. Pines and J.S. Waugh, J. Chem. Phys., 59, 591 (1973).
5. M. Luzar, V. Rutar, J. Seliger and R. Blinc, to appear in Ferroelectrics.
6. D.L. Van der Hart, J. Chem. Phys., 64, 830 (1976).
7. H.S. Gorslow, J.S. Jaeger, Conduction of Heat in Solids, Oxford Univ. Press, London, 1959.
8. G. Chidichimo, Z. Yaniv, N.A.P. Vaz, and J.W. Doane, Phys. Rev. A, 25, 1077 (1982).
9. Z. Yaniv, G. Chidichimo, N. Vaz, J.W. Doane, Phys. Lett., 86A, 297 (1981).